Temporal evolution of measured climate forcing agents at South Pole, Antarctica

Sachin D. Ghude[1], S. L. Jain[2,*] and B. C. Arya[2]

[1]Indian Institute of Tropical Meteorology, Pune 411 008, India
[2]Radio and Atmospheric Sciences Division, National Physical Laboratory, New Delhi 110 012, India

Greenhouse gas (GHG; mainly CO_2, CH_4, N_2O, CFC-11 and CFC-12) measurements for 22 years (1983–2004) have been analysed to evaluate the radiative forcing (RF) and temporal evolution at the South Pole. About 20% increase in growth rate of CO_2 has been observed during 1992–2004 compared to 1983–91. However, remarkable deceleration in the growth rate of CH_4, CFC-11 and CFC-12 has been observed. CO_2 radiative forcing has increased by ~49% during 2004 for 10% increase in CO_2 concentration during the last 22 years. RF due to CH_4 was found to be 0.47 Wm^{-2} in 1999 and since then has remained almost constant through 2004. The net RF has been observed to increase by 0.7 Wm^{-2} during 2004 compared to 1983, which corresponds to ~38% increase in the last 22 years. Growth rate of net RF decreased by ~22% during 1990–2004, compared to the growth rate during 1983–90. A global warming simulation made using the EdGCM model shows an increase in surface air temperature and sea surface temperature of about 1.7°C and 1°C respectively, in 2050 compared to 1958. In response to change in GHGs from 1958 to 2050, warming over the higher latitudes is greater than in the tropics and also increase in minimum temperature is greater than the increase in maximum temperature. Similarly, up to 50% change in snow–ice cover over some of the regions in the higher latitudes is observed with this simulation.

Keywords: EdGCM model, global warming, greenhouse gases, radiative forcing.

INCREASE in the atmospheric concentration of greenhouse gases (GHGs) such as CO_2, CH_4, N_2O, tropospheric ozone, CFCs, etc. since the industrial period (1750) has been identified as a major cause of the warming of the earth's surface and climate change[1–5]. The concentration of atmospheric methane (CH_4) has almost tripled since pre-industrial times in response to rice cultivation, livestock breeding and extraction of coal and natural-gas resources. Tropospheric ozone has recently increased sharply regionally, adding to regional warming[6]. Decreasing stratospheric ozone affects radiative forcing (RF) causing climate change and also affects the climate by modifying stratospheric dynamical processes.

Increasing anthropogenic GHGs cause the largest positive forcing and their concentrations are analysed in terms of the changes in RF since 1750 (pre-industrial concentrations)[7]. The perturbation to radiative climate forcing related to long-lived and nearly homogeneously distributed (around the globe) GHGs has the largest magnitude and least uncertainty[1,5,7]. A remarkable deceleration in the growth rate of some of the GHG climate forcing agents has occurred in the past 20 years[8–11]. The growth rate of climate forcing by measured GHGs has declined to 3 Wm^{-2} $century^{-1}$ from almost 5 Wm^{-2} $century^{-1}$, which was at a peak[9] in 1980. This slowdown is caused largely due to the phase-out of CFCs because of cooperative international action and because of flattering of the CO_2 growth rate, which is related to the slower growth rate of fossil fuel CO_2 emission[9]. Another factor[12,13] was the slowdown in the growth rate of CH_4. The CH_4 growth rate observed by Dlugokencky and co-workers[14,15] was below the IPCC estimate. The present findings suggest that CH_4 forcing growth rate may turn negative sooner than that of the IPCC (2001) projection[10,16]. While increasing CO_2 causes the largest positive RF now and is likely to be the dominant forcing in future, the estimated[1,7,9,10] CH_4 forcing is half that of CO_2. Moreover, the sum of all forcing components (other than CO_2) is as much as that of CO_2 alone. Therefore, knowledge of each of the large forcing components is needed to obtain the realistic rates of warming and heat storage in the ocean. Although the current trend of climate forcing by aerosols remains uncertain and negative forcing due to aerosol (except black carbon) may lead to less global warming than predicated, understanding the forcing trend due to GHGs is vital for development of effective policies.

In this article we have calculated the trend of climate forcing by measured changes in GHGs (mainly CO_2, CH_4, N_2O, CFC-11 and CFC-12) with data taken from the South Pole (assuming that it represents the background concentration of the GHGs). We have used measured changes in GHG concentration and likely trend in future GHGs to run a global warming simulation using the NASA EdGCM model.

*For correspondence. (e-mail: sljain@nplindia.ernet.in)

Method

Observational data

The GHG data from the South Pole, Antarctic research station have been used in the present study. These data have been taken from the website of the World Meteorological Organization (WMO), Global Atmospheric Watch (GAW), World Data Center for Greenhouse Gases (WDCGG). This site is maintained by the Japan Meteorological Agency (JAM) in cooperation with the WMO. The GAW programme of WMO promotes systematic and reliable observations of the global atmospheric environment, including measurements of several trace gases. The measurement data are reported by participating countries, and archived and distributed by the WDCGG at JAM. A detailed description of the instrument and measuring procedure can be found at http://gaw.kishou.go.jp/wdcgg.html.

Radiative forcing calculations

In the present study, RF was calculated as the difference between irradiance in the pre-industrial and present-day atmosphere due to changes in the concentration of globally mixed GHGs[17]. The recommended expressions to convert GHG changes relative to 1750 to instantaneous RF are given by Myher *et al.*[7] and Harvey *et al.*[18] (Table 1). To calculate the RF due to CO_2, CH_4, N_2O, CFC-11 and CFC-12, we have used a simple mathematical relationship as formulated by Myher *et al.*[7]. The mathematical relationships for calculating RF due to indirect CH_4 forcing (O_3 and stratospheric H_2O formational due to CH_4 build-up) are taken from Harvey *et al.*[18]. Contrary to climate models, these results are based mainly on measurements and have relatively high precision.

NASA EdGCM model

The EdGCM model gives a research-quality global climate model (GCM) wrapped in a graphical user interface that runs on a desktop computer, unlike GCM which runs on a workstation. The climate model used by the EdGCM software was developed at the Goddard Institute for Space Studies (GISS), NASA. This type of 3D computer model is known as a grid-point GCM. The EdGCM model has 7776 grid cells in the atmosphere, with each horizontal column corresponding to 8° latitude by 10° longitude, and containing nine vertical layers. The EdGCM software allows designing of the experiment, running simulations, post-processing and analysing data using scientific visualization for data display. The trend section in the model can create complex input trends for any/all of the major GHGs (CO_2, CH_4, N_2O, CFC-11 and CFC-12). More details can be found at http:// EdGCM.columbia.edu.

Results and discussion

Temporal evolution of GHG trend at South Pole

The available monthly mean station data for CO_2, CH_4, N_2O, CFC-11 and CFC-12 have been used to calculate the yearly average. The temporal evolution of long-lived GHGs at the South Pole and year-to-year changes from 1983 to 2004 are displayed in Figures 1 and 2 respectively. CO_2 concentration had increased linearly since 1983, which corresponds to ~10% increase in 2004. The annual growth of CO_2 concentration has been observed to be relatively flat (1.57 (±0.75) ppm) since the last 22 years. The flat growth rate suggests either a net increase in the uptake of CO_2 by terrestrial sinks and/or ocean, or reduction in CO_2 emission. Hansen and Sato[9] reported that fossil-fuel CO_2 emissions during the last three decades have increased at about 1% per year. This implies that the net increase in uptake of CO_2 by terrestrial sinks and/or ocean has increased during the past three decades. However, in reality, the growth rate of CO_2 has increased from 1.50 (±0.26) ppm yr^{-1} during 1983–91 to 1.8 (±0.3) ppm yr^{-1} during 1992–2004, which corresponds to 20% increase in the growth rate. Large annual increase in CO_2 concentration (2.43 ppm) occurred in 1998, whereas minimum increase in CO_2 concentration (0.88 ppm) occurred in 1993. Fluctuations of this kind have also been reported by other investigators[1,9,10]. Close examination of the growth rate (linear fit) revealed that it is increased at about 0.030 ppm yr^{-1} during the past 22 years. In reality, CO_2 growth rate decreased by about 0.023 ppm yr^{-1} during 1984–91 period increased by about 0.067 ppm yr^{-1} during 1992–2004. In addition to CO_2, N_2O continues to increase linearly with an average rate of 0.71 ppb yr^{-1} (1983–2004) and shows almost flat growth rate.

As seen in Figures 1 and 2, a remarkable decrease in the growth rate of CH_4, CFC-11 and CFC-12 has been observed. CH_4, which has a climate forcing half that of CO_2, has been observed almost constant at ~1730 ppb since 1999, suggesting that methane concentration for this six-year period is almost at steady state. Measurements made at the Indian research station, Maitri, Antarctica, also showed steady state concentration of methane[19]. Yearly average of CH_4 which was ~1580 ppb during 1983 has increased to ~1730 ppb in 1999, corresponding to ~10% increase and has since remained essentially constant through 2004. Though CH_4 concentration has increased ~10% during the past 22 years, its growth has decreased from 11.62 ppb yr^{-1} averaged for 1983–91 to 5.4 ppb yr^{-1} averaged for 1992–99, corresponding to about ~55% reduction and was near zero through 1999–2004. A close examination of the growth rate (linear fit), however, revealed that it has decreased at an average rate of about 0.67 ppb yr^{-1} during the last 22 years. The cause of this is likely linked to changes in the emission in the former Soviet Union, reduced growth rate of CH_4 sources, and the

Table 1. Mathematical formulas used to estimate the radiative forcing

Trace gas	Simplified expression radiative forcing, ΔF, Wm^{-2}
CO_2	$\Delta F = \alpha \ln (C/C_0)$, (where $\alpha = 5.35$)
CH_4	$\Delta F = \alpha (\sqrt{M} - \sqrt{M_0}) - (f(M, N_0) - f(M_0, N_0)$, (where $\alpha = 0.036$)
N_2O	$\Delta F = \alpha (\sqrt{N} - \sqrt{N_0}) - (f(M_0, N) - f(M_0, N_0)$, (where $\alpha = 0.1.2$)
CFC-11	$\Delta F = \alpha (X - X_0)$, (where $\alpha = 0.25$)
CFC-12	$\Delta F = \alpha (X - X_0)$, (where $\alpha = 0.33$)
Stratospheric water vapour	$\Delta F = 0.05\ \Delta FCH_{4-pure}$
Tropospheric ozone	$\Delta F = 8.62 \times 10^{-5}\ \Delta C_{CH_4}$ for O_3 formation due to CH_4 buildup

Notes: where $f(M, N) = 0.47$ in$[1 + 2.01 \times 10^{-5}\ (MN) + 5.31 \times 10^{-5}\ M(MN)^{1.52}]$ (correction to the CH_4 forcing due to overlap with N_2O and correction to the N_2O forcing due to overlap with CH_4).
C is CO_2 in ppmv at time t and C_0 is the pre-industrial concentration.
M is CH_4 in ppbv at time t and $[CH_4]_0$ is the pre-industrial concentration.
N is N_2O in ppbv at time t and $[N_2O]_0$ is the pre-industrial concentration.
X is CFC in ppbv at time t and X_0 is the pre-industrial concentration.
$\Delta FCH_{4\text{-pure}}$ is methane forcing before correction for overlap with N_2O.
ΔC_{CH_4} is change in methane concentration at time t compared to its pre-industrial concentration.

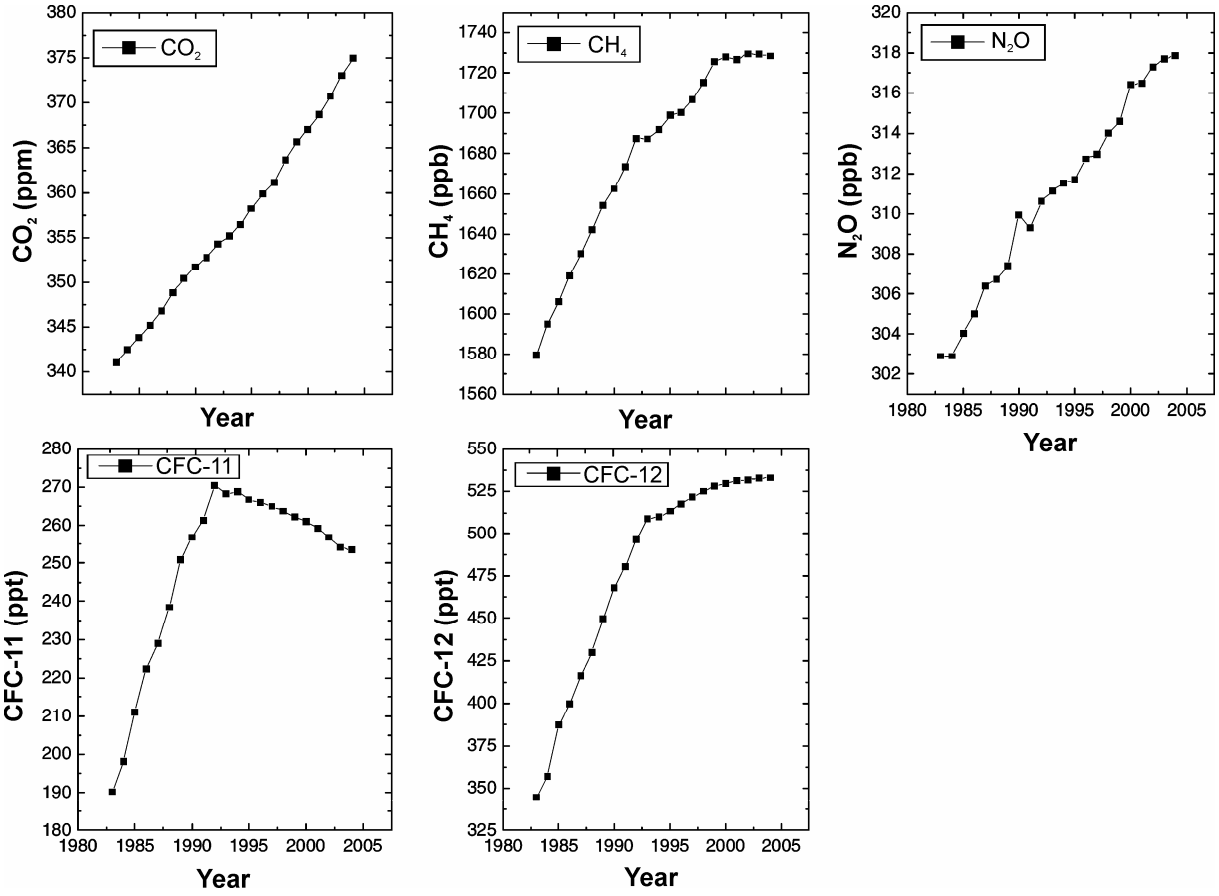

Figure 1. Temporal evolution of greenhouse gas concentration at the South Pole during 1983–2004.

short lifetime of CH_4, resulting in a pseudo-equilibrium between sources and sinks of this timescale, including several other factors[13–15,17]. CFC-11 and CFC-12 have increased from their nearly zero concentrations in 1950 to 253 ppt and 533 ppt respectively, in 2004. Though CFC-11 and CFC-12 concentrations have increased by 33% and 55% during the past 22 years, their growth has ceased to increase around 1992. The average growth rate of CFC-11 which was 9 ppt yr^{-1} for 1983–92 turned out to be negative, about –1.4 ppt yr^{-1} average for 1993–2004. The average growth rate of CFC-12 was 17 ppt yr^{-1} for 1983–92. Since 1992, the growth rate of CFC-12 started to decrease and reached near zero in 2004. This implies that the growth rate of CFC-11 had already turned negative in

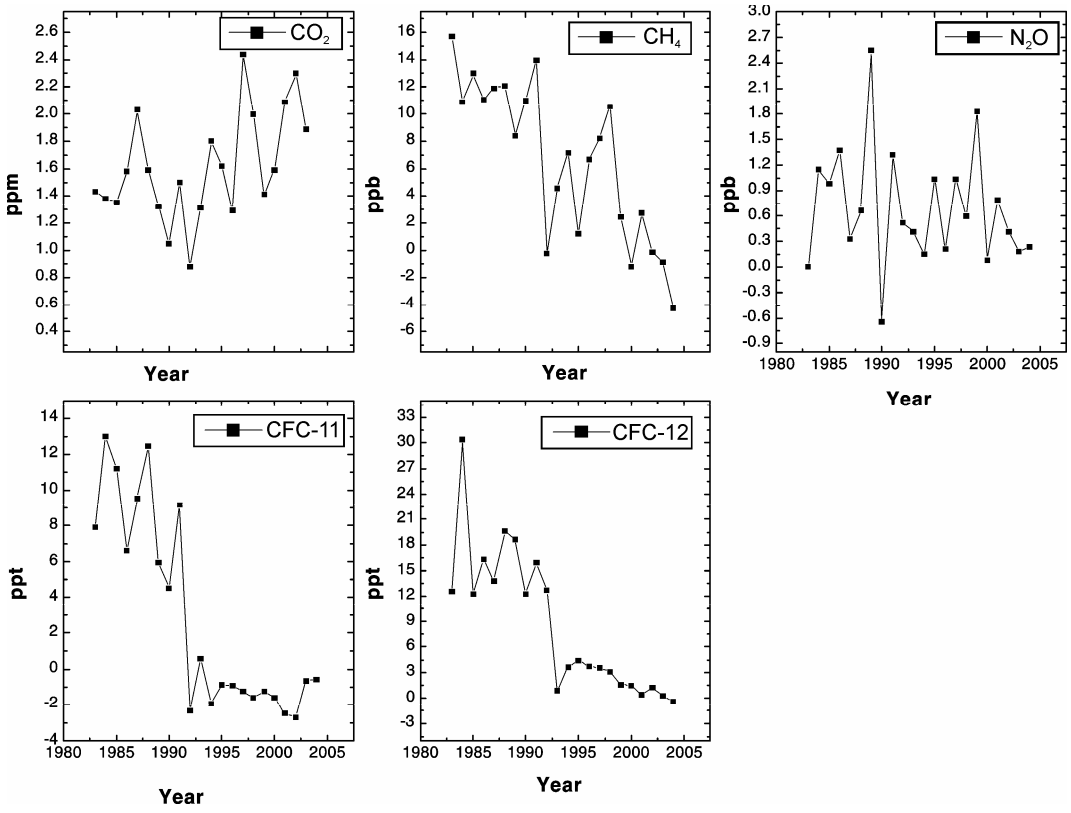

Figure 2. Year-to-year change in GHG concentration at the South Pole during 1983–2004.

the mid-1990s and that of CFC-12, which is now nearly zero, will be negative in the future as a result of restrictions imposed on production by the Montreal Protocol.

Temporal evolution of radiative forcing

Temporal evolution of RF due to CO_2, CH_4, N_2O, CFC-11 and CFC-12 during 1983–2005 is shown in Figure 3. We also associate with CH_4 its indirect effects on tropospheric O_3 and stratospheric H_2O build-up, highlight the importance of CH_4 as a climate forcing. Trends of the climate forcing are revealed better by their instantaneous annual growth rates (Figure 4). The RF due to CO_2 compared to its pre-industrial concentration was 1.05 Wm^{-2} in 1983. The CO_2 RF increased to 1.56 Wm^{-2} during 2004, which corresponds to ~49% increase due to 10% increase in CO_2 concentration since the last 22 years. The growth rate of CO_2 RF was relatively flat and averaged 0.023 (±0.005) Wm^{-2} yr^{-1} or 2.3 Wm^{-2}/century over the last 22 years. Earlier studies have shown that the growth rate of CO_2 RF almost doubled between the 1950s and 1970s. However, it was flat from 1980 until late 1990s, despite 30% increase in fossil fuel[9]. The recent approximate flat growth rate as observed in Figure 3 despite continuing increase in CO_2 emission at about 1.2% per year since 1975 implies that terrestrial and/or oceanic sinks may have increased during this period. However, second-order polynomial fit on the CO_2 RF growth rate as shown in Figure 4, in reality shows that the CO_2 RF growth rate decreased from 1983 to 1992 and since 1992 it has been increasing at a rate of 0.09 Wm^{-2}/century. In addition to CO_2, RF due to N_2O was observed to be 0.110 Wm^{-2} in 1983, which increased to 0.158 Wm^{-2} in 2004. This corresponds to ~44% increase in RF for 5% increase in N_2O concentration since the last 22 years.

A dramatic RF change occurred for CH_4 (Figure 3). RF due to CH_4 increased from about 0.42 Wm^{-2} during 1983 to 0.47 Wm^{-2} during 1999. Since then CH_4 RF remained essentially constant through 2004. A 10% increase in CH_4 concentration has caused 14% increase in CH_4 RF since the past 22 years. When compared to the increase in RF due to CO_2 during the last 22 years, CO_2 RF was found to increase about ten times than CH_4 RF. Though CH_4 RF showed 14% increase since the last 22 years, large year-to-year variations in RF occurred and it decreased to zero recently, as shown in Figure 4, which displays the instantaneous change of CH_4 RF for the past 22 years. In addition, indirect CH_4 RF due to O_3 and stratospheric H_2O built up due to CH_4 have been observed to cause additional 25% RF forcing than that of CH_4. Indirect CH_4 RF increased from 0.10 Wm^{-2} during 1983 to 0.12 Wm^{-2} in 2004. However, as expected, it followed a similar trend as observed in CH_4. This corresponds to 20% increase in

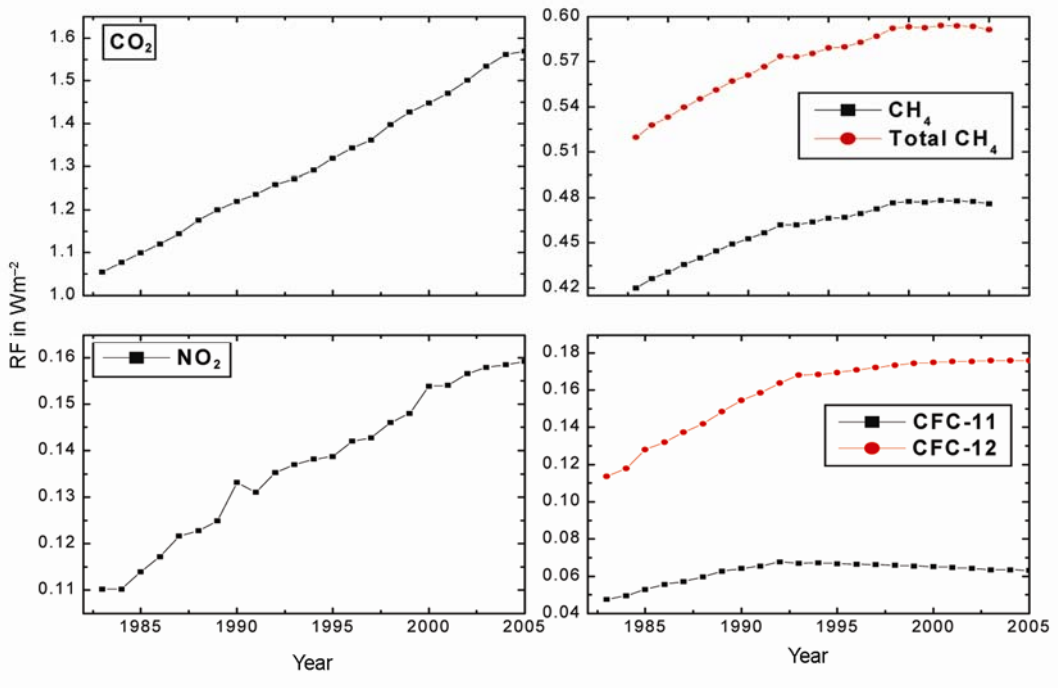

Figure 3. Temporal evolution of radiative forcing (RF; Wm^{-2}) at the South Pole during 1983–2004.

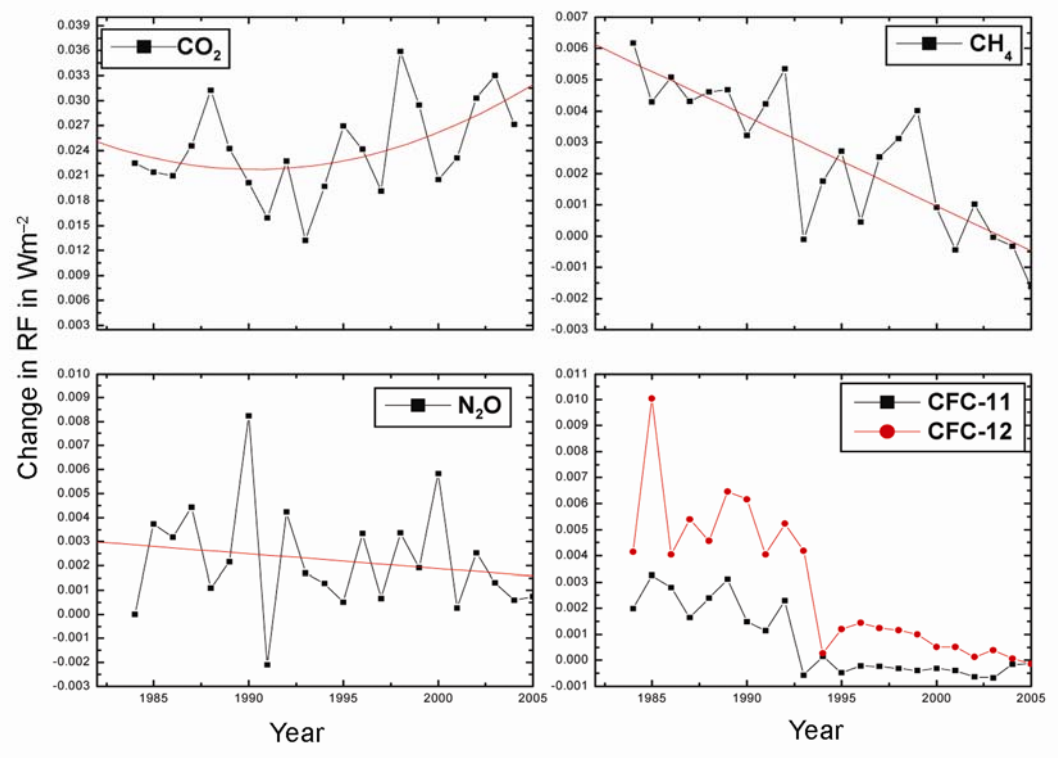

Figure 4. Year-to-year change in RF (Wm^{-2}) at the South Pole during 1983–2004.

indirect CH_4 RF for 10% increase in methane concentration for the past 22 years.

In addition to CH_4, growth of CFC (CFC-11 and CFC-12) RF has been decreasing since 1992, two years after the Kyoto Protocol baseline year. RF due to CFC-11 and CFC-12 increased from 0.048 and 0.113 Wm^{-2} in 1983 to 0.063 and 0.176 Wm^{-2} in 2004 respectively. In reality, CFC-11 increased 42% during 1983–92 at a rate of

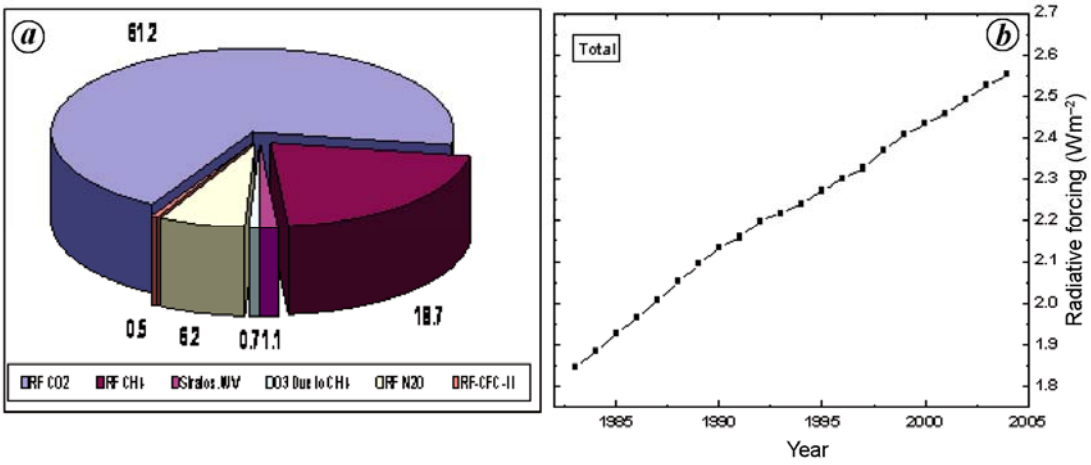

Figure 5. ***a***, Percentage contribution of individual RF to total RF due to GHGs during 2004. ***b***, Temporal evolution of total RF trend from 1983 to 2004.

~0.23 Wm^{-2}/century and recently, decreased by about 6% from 1992 at a rate of 0.04 Wm^{-2}/century. Similarly, CFC-12 increased 48% during 1983–93 at a rate of ~0.55 Wm^{-2}/century. However, CFC-11 increased only about 5% from 1993 to 2004, and the growth rate has decreased to an averaged value of 0.08 Wm^{-2}/century since the last 13 years. Available records of CFC-113 show that the CFC-113-induced RF decreased from 0.030 Wm^{-2} in 1996 to 0.029 Wm^{-2} in 2004, at a rate of 0.02 Wm^{-2}/century. This corresponds to ~3% decrease in CFC-113 RF for about 8% decrease in CFC-113 concentration for the last eight years. The remarkable decline in CFC RF since 1992 is because of the restriction imposed by the Montreal Protocol. These observations suggest that the net change in CFC RF in the next 50 years will be small.

Trend of net climate forcing

Figure 5 *a* shows the percentage contribution of individual RF to total RF due to CO_2, CH_4 (total), CFC (11 and 12) and N_2O during 2004. Maximum contribution of about 61% in total RF has been observed due to CO_2. Contribution due to CH_4 and CFC (11 and 12) to the net RF has been observed to be ~32.6% and found to be decreased by 5% in 2004, compared to 1983. Figure 5 *b* shows the temporal evolution of total RF trend from 1983 to 2004. The net RF increased from 1.85 Wm^{-2} in 1983 to 2.55 Wm^{-2} in 2004. This increase of about 0.7 Wm^{-2} observed in the last 22 years has caused ~38% increase in the net RF in 2004, at an average rate of ~3.3 Wm^{-2}/century. In reality, net RF increased at a rate of 4.1 Wm^{-2}/century from 1983 to 1990 and reduced to 3 Wm^{-2}/century from 1990 (Kyoto Protocol baseline year) to 2004. This corresponds to 22% decrease in growth rate of net RF for the period 1990–2004.

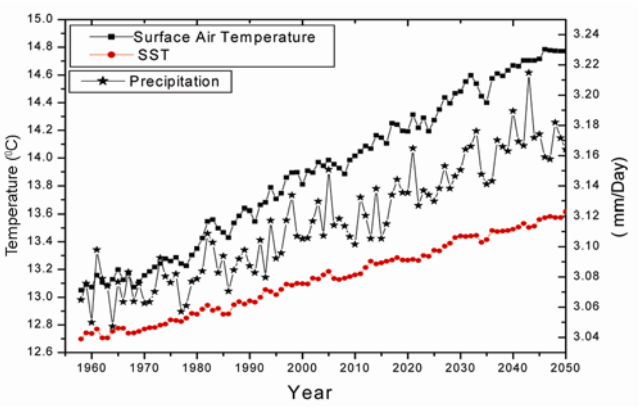

Figure 6. Temporal evaluation of simulated global mean surface air temperature, sea surface temperature and precipitation (mm/day) for 1958–2050.

Global warming (climate model prediction)

A global warming simulation has been made with the EdGCM model to study the effects of changing GHG concentration on the earth's climate. We have used observed changes in GHG concentration and likely trend in future GHG for the next 50 years (proposed by Hansen *et al.*[9]) to run the global warming simulation, which begins in 1958 and ends in 2050. We have used observed changes in atmospheric CO_2 and N_2O concentration for 1958–2004 and allowed it to increase at a projected rate of 1.8 ppm/yr and 0.70 ppb/yr till 2050. Our approach of using projected rate of increase of CO_2 and N_2O is based on the observed emission trend during the last 10 years. Similarly, for CH_4, CFC-11 and CFC-12, we have used observed year-to-year changes per year in their growth rate till 2004. However, we allowed a decrease in CH_4 at the rate of 0.5% per year, and CFC-11 and CFC-12 at the rate

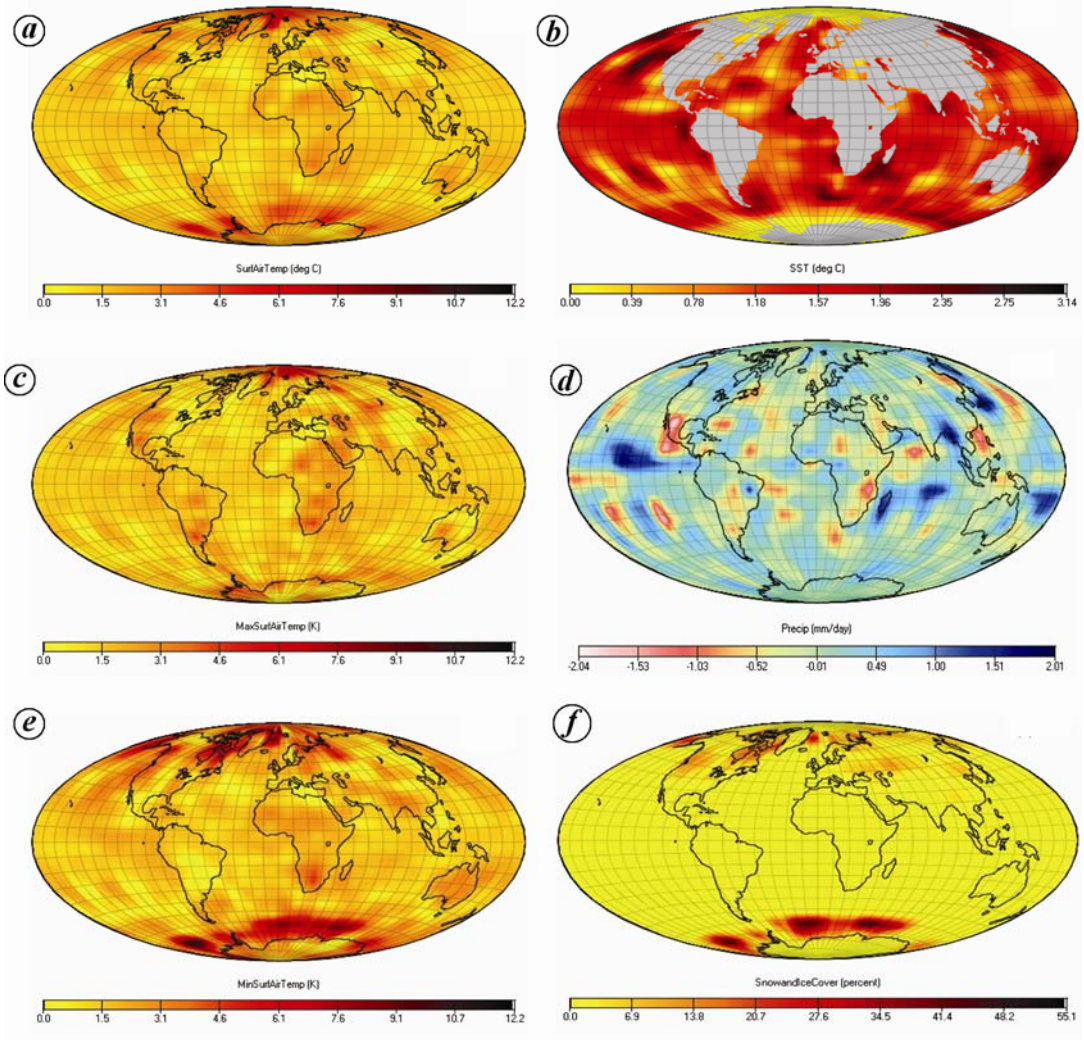

Figure 7. Geographical distribution of changes in different climate parameters during 2004 compared to 1958 as simulated by EdGCM.

of 1% per year from 2005 (ref. 9). Initial conditions, boundary conditions, GHG concentrations from 1958 to 1983 and solar luminosity were set to default values given for the global warming simulation with EdGCM.

Figure 6 shows the temporal evaluation of simulated global mean surface air temperature (SAT), sea surface temperature (SST) and precipitation (mm/day) for 1958–2050. The global warming simulation (based on the 1958 climate) for SAT and SST was about 13°C and 12.7°C respectively, while at the end of the simulation year (2050), the values were about 14.7°C and 13.6°C respectively, in response to the GHG trend discussed above. Similarly, simulated global mean precipitation during 1958 was about 3.07 mm/day, while at the end of simulation it was 3.18 mm/day. Therefore, global warming of 1.7°C in SAT and 1°C in SST will occur in 2050 for this simulation. However, as can be seen from Figure 6, only 0.1 mm/day increase in global average precipitation will occur in 2050. Plotting the difference between the 1958 and 2050 values for SAT, SST, precipitation and snow-ice cover will show the increase/decrease in these climate parameters in response to the change in GHG used in this global warming simulation. As can be seen from Figure 7, warming (SAT (average, maximum and minimum)) has not been geographically uniform. Although the simulation shows warming all over the region, it was greater over some of the land and ice-covered areas than the ocean. Warming over higher latitudes was greater than in the tropics and also increase in minimum temperature was greater than the increase in maximum temperature. Similarly, warming in the sea surface mixed layer was also observed all over the ocean; however, increase in temperature was greater over some regions than others. In addition, the geographical distribution of change in precipitation (2050–1958) showed non-uniform distribution of precipitation (mm/day). In response to change in GHGs used in this simulation, precipitation was found to decrease in majority of the tropical regions. However, it increased

in some of the tropical regions. Therefore, the net increase observed in Figure 6 shows negligible increase in global precipitation.

One key element for the geographical distribution of global warming is related to ice-albedo feedback mechanism. Figure 7 *f* shows the geographical distribution of the percentage change in snow-ice cover change in 2050 (1958–2050). Up to 50% change in snow-ice cover was seen over the higher latitudes. This change in snow-ice cover was found to be highly correlated with increase in SAT, more notable over the coastal Antarctic region. Ice-albedo feedback mechanism is related to the fact that as the climate warms, snow and ice begin to melt. As they melt, the underlying surface reflects far less of the solar radiations than the high reflection snow–ice surface. The surface absorbs more energy and warms more than the surrounding region, further melting the snow and ice cover.

Conclusion

We have analysed temporal evolution of GHGs (mainly CO_2, CH_4, N_2O, CFC-11 and CFC-12) at the South Pole for 1983–2004. We have also calculated the RF due to measured changes in CO_2, CH_4, N_2O, CFC-11 and CFC-12 compared to its pre-industrial concentration. Approximately 10% increase in CO_2 concentration has been observed compared to the 1983 concentration. About 20% increase in the growth rate of CO_2 was observed during 1992–2004 compared to 1983–91. Growth of CO_2 was observed to be 1.8 (±0.3) ppm/yr during 1992–2004. About 5% increase in N_2O observed in 2004, shows almost a flat growth rate of N_2O of about 0.71 ppb/yr since 1983. Remarkable deceleration in the growth rate of CH_4, CFC-11 and CFC-12 has been observed. Concentration of CH_4 was observed to be almost constant at ~1730 ppb since 1999, suggesting that methane concentration for this six-year period was almost at steady state. CH_4 growth has decreased from 11.62 ppb/yr average for 1983–91 to 5.4 ppb/yr average for 1992–99, corresponding to about ~55% reduction and was near zero during 1999–2005. Growth rate of CFC-11 and CFC-12, which averaged 9 and 17 ppt yr^{-1} for 1983–92 turned negative to about –1.4 ppt yr^{-1} and was near zero when averaged for 1993–2004.

The RF due to CO_2 increased to 1.56 Wm^{-2} during 2004 corresponding to ~49% increase due to 10% increase in CO_2 concentration since the last 22 years. RF due to N_2O also increased to 0.158 Wm^{-2} in 2004, which corresponds to ~44% increase in RF for 5% increase in N_2O concentration since the last 22 years. RF due to CH_4 was observed to be 0.47 Wm^{-2} in 1999 and since then has remained almost constant through 2004. A 10% increase in CH_4 concentration caused 14% increase in CH_4 RF during the past 22 years. Indirect CH_4 RF due to O_3 and stratospheric H_2O built up due to CH_4 has been observed to cause additional 25% RF forcing and was found to be about 0.12 Wm^{-2} in 2004. RF due to CFC-11 and CFC-12 was observed to be 0.063 and 0.176 Wm^{-2} in 2004 respectively. The remarkable decline in CFC RF since 1992 is because of restriction imposed by the Montreal Protocol (40). These observations suggest that the net change in CFC RF in the next 50 years will be small. The net RF compared to its pre-industrial concentration was found to be around 2.55 Wm^{-2} during 2004 due to CO_2, CH_4 (direct + indirect), N_2O, CFC-11 and CFC-12. An increase of about 0.7 Wm^{-2} has been observed since the last 22 years, which caused ~38% increase in GHG-induced RF. About 22% decrease in growth rate of net RF during 1990–2004 has been observed with respect to the observed growth rate during 1983–1990. This slowdown was caused mainly by the Montreal Protocol phase-out of ozone-depleting gases. It was accomplished by means of cooperative and not punitive, international actions.

A global warming simulation has been made with the EDGCM model to simulate the effects on climate of changing GHG concentration, from 1958 to 2050. The simulation shows global warming with increase in SAT and SST of 1.7°C and 1°C respectively, in 2050 compared to 1958. However, negligible increase in global average precipitation of about 0.1 mm/day was observed in 2050. In response to change in GHGs from 1958 to 2050, geographical distribution shows warming all over the region; however, this was not uniform. Warming over the higher latitudes was greater than in the tropics and also increase in minimum temperature was greater than the increase in the maximum temperature. Geographical distribution of change in precipitation also showed non-uniform distribution. Precipitation was found to decrease in majority of the tropical region. However, it also showed an increase in some of the tropical regions. Up to 50% change in snow–ice cover over some of the regions in the higher latitudes was seen.

Current trend and projections of climate forcing lead us to predict global warming for several decades at a rate of 0.2 ± 0.06°C per decade. Higher latitudes will experience more warming than any other regions. It is now impossible to avoid global warming for the next 50 years. However, actions outlined by the Montreal and Kyoto protocols can slowdown global warming. This conclusion supports the need for actions that slow down the growth of climate forcing.

1. Intergovernmental Panel on Climate Change (IPCC). In *Climate Change 2001: The Scientific Basis* (eds Houghton, J. T. *et al.*), Cambridge University Press, New York, 2001.
2. Hansen, J. E., Sato, M., Lacis, A., Ruedy, R., Gegen, I. and Matthews, E., Climate forcing in the industrial era. *Proc. Natl. Acad. Sci. USA*, 1998, **95**, 12753–12758.
3. Lacis, A., Hansen, J., Lee, P., Mitchell, T. and Lebedeff, S., Greenhouse effect of trace gases 1970–1980. *Geophys. Res. Lett.*, 1981, **8**, 1035–1038.

4. Wang, W. C., Yung, Y. L., Lacis, A. A., Mo, T. and Hansen, J. E., Greenhouse effects due to man-made perturbation of trace gases. *Science*, 1976, **194**, 685–690.
5. Jain, A. K., Briegleb, B. P., Minschwaner, K. and Wuebbles, D. J., Radiative forcing and global warming potentials of 39 greenhouse gases. *J. Geophys. Res*., 2000, **105**, 20773–20790.
6. Akimoto, H., Global air quality and pollution. *Science*, 2003, **302**, 1716–1719.
7. Myhre, G., Highwood, E. J., Shine, K. P. and Stordal, F., New estimates of radiative forcing due to well mixed greenhouse gases. *Geophys. Res. Lett*., 1998, **25**.
8. Intergovernmental Panel on Climate Change (IPCC), In *IPCC Guidelines for National Greenhouse Gas Inventories, Prepared by the National Greenhouse Gas Inventories Programme* (eds Eggleston, H. S. *et al.*), IGES, Japan, 2006.
9. Hansen, J. E. and Sato, M., Trends of measured climate forcing agents. *Proc. Natl. Acad. Sci. USA*, 2001, **98**, 14778–14783.
10. Hansen, J. E., Sato, M., Ruedy, R., Lacis, A. and Oinas, V., Global warming in the twenty-first century: An alternative scenario. *Proc. Natl. Acad. Sci. USA*, 2000, **97**, 9875–9880.
11. Hansen, J. E., Sato, M., Glascoe, J. and Ruedy, R., A common-sense climate index: Is climate changing noticeably? *Proc. Natl. Acad. Sci. USA*, 1998, **95**, 4113–4120.
12. Lelieveld, J. and Crutzen, P. J., Indirect chemical effects of methane on climate warming. *Nature*, 1992, **355**, 339–342.
13. Lelieveld, J., Crutzen, P. and Dentener, F. J., Changing concentration, lifetime and climate forcing of atmospheric methane. *Tellus*, 1998, **B50**, 128–150.
14. Dlugokencky, E. J., Walter, B. P., Masarie, K. A., Lang, P. M. and Kasischke, E. S., Measurements of an anomalous global methane increase during 1998. *Geophys. Res. Lett*., 2001, **28**, 499–502.
15. Dlugokencky, E. J., Houweling, S., Bruhwiler, L., Masarie, K. A., Lang, P. M., Miller, J. B. and Tans, P. P., Atmospheric methane levels off: Temporary pause or a new steady-state? *Geophys. Res. Lett.*, 2003, **30**, 1992.
16. Dlugokencky, E. J., Masarie, K. A., Tans, P. P., Conway, T. L. and Xiong, X., Is the amplitude of the methane seasonal cycle changing? *Atmos. Environ.*, 1997, **31**, 21–26.
17. Intergovernmental Panel on Climate Change (IPCC), *Climate Change 1995: The Science of Climate Change*, Contribution of working group I to the second assessment report of the IPCC, Cambridge University Press, UK, 1995.
18. Harvey, L. D. D. *et al.*, An introduction to simple climate models used in the IPCC second assessment report. IPCC Technical Paper 2, 1997, p. 50.
19. Jain, S. L., Ghude, S. D., Ashok, K., Arya, B. C., Kulkarni, P. S. and Bajaj, M. M., Continuous observations of surface air concentration of carbon dioxide (CO_2) and methane (CH_4) at Maitri, Antarctica. *Curr. Sci.*, 2005, **88**, 1941–1948.

ACKNOWLEDGEMENTS. We thank GISS, NASA, Mark Chandler and Linda E. Sohl for making available the EdGCM tool. We also thank JAM and WMO for making available GHG data (http://gaw.kishou.go.jp/wdcgg.html). S.L.J. thanks CSIR, New Delhi for providing financial support under the CSIR Emeritus Scientist Scheme.

Received 4 December 2007; revised accepted 23 October 2008